Peer-reviewed version available at Energies 2019, 12, 544; doi:10.3390/en12030544

Article

FAST PROCESSING INTELLIGENT WIND FARM CONTROLLER FOR PRODUCTION MAXIMISATION

Tanvir Ahmad [1,2]*, Abdul Basit [1], Samia Akhtar [3], Juveria Anwar [1], Olivier Coupiac [4], Behzad Kazemtabrizi [2] and Peter C Matthews [2,]

[1] US Pakistan Center for Advanced Studies in Energy, UET Peshawar Pakistan
[2] School of Engineering Durham University, UK
[3] Pakistan Council of Renewable Energy Technologies
[4] Engie Green France
* Correspondence: tanvir.ahmad@uetpeshawar.edu.pk

Version January 8, 2019 submitted to Preprints

Abstract: A practical wind farm controller for production maximisation based on coordinated control is presented. The farm controller emphasises computational efficiency without compromising accuracy. The controller combines Particle Swarm Optimisation (PSO) with a turbulence intensity based Jensen wake model (TI-JM) for exploiting the benefits of either curtailing upstream turbines using coefficient of power (C_P) or deflecting wakes by applying yaw-offsets for maximising net farm production. First, TI-JM is evaluated using convention control benchmarking WindPRO and real time SCADA data from three operating wind farms. Then the optimized strategies are evaluated using simulations based on TI-JM and PSO. The innovative control strategies can optimise a medium size wind farm, Lillgrund consisting of 48 wind turbines, requiring less than 50 seconds for a single simulation, increasing farm efficiency up to a maximum of 6% in full wake conditions.

Keywords: wind farm production maximisation, coordinated control, C_P-based optimisation, yaw-based optimisation, wake effects, turbulence intensity, Jensen model, particle swarm optimisation

1. Introduction

Wind farms take advantages of economies of scale for reducing levelised cost of energy by clustering turbines together. However, turbines in this cluster interact with each other aerodynamically through wake effects. Wake effects or simply wakes can significantly impact economic performance of a wind farm by decreasing net production or increasing fatigue loads [1–3].

Industry best practice is to increase the spacing between the turbines in the prevailing wind directions (downwind) as compared to non-prevailing wind directions (crosswind) [2]. Wake losses in the crosswind directions can be as high as 50% due to the close spacing [4], reducing the farm efficiency to as low as 40% [5].

Another way of reducing wake effects is global optimisation of the whole wind farm using coordinated control. With state of the art (greedy control), every turbine maximises its own production, neglecting the wake effects on shadowed turbines [2]. Coordinated control based on global optimisation of the whole wind farm instead of local optimisation of individual turbines can result in increased annual energy production [6].

Coordinated control is the farm level control (termed farm control or optimised control as well), which is based on the optimised cooperation or coordination of turbines in the farm. In such control, turbines coordinate with each other for increasing the net production. Curtailing or yawing the upstream turbines reduces the wake effects produced, hence increasing production of downstream turbines. If decrease in the upstream turbines' net production is less than increase in the downstream turbines' net production then the farm net production will increase.

A detailed literature review of coordinated control studies in [7,8] concludes that realisation of benefits of coordinated control depends upon terrain characteristics, atmospheric wind conditions, layout of the wind farm and number of turbines under consideration. Wakes recover quickly in rough terrains as compared to smooth surfaces (offshore) [7]. In certain wind directions, downstream turbines are under significant wake effects, impacting their production negatively. Usually negligible wake effects are observed at higher wind speeds in above-rated wind conditions [5]. Net production of denser wind farms (with closely spaced turbines) is generally affected more by wake effects [5].

Coordinated control can be performed with optimal settings of C_P or yaw offsets (α) of the upstream turbines. This requires no additional cost, where the only change required in the existing control system will be the coordinated control algorithm, specifically a change in the software [4,9]. Intelligent farm control aimed at maximising net present value will replace turbine power curve as the main performance characteristic [6]. As real time on-line optimisation is required and given the stochastic nature of wind, the controller must be fast and accurate. Specifically, control updates need to be made in seconds. An optimiser and a wind deficit model (wake model) are required in such setup for coordinated control. The optimiser evaluates different combinations of power productions of the turbines using the wind deficit model for achieving the optimum net production. It shall be noted that there is an inverse relationship between accuracy and computational cost of the farm controller. Real time (online) implementation of coordinated control requires faster (usually in the order of seconds) and accurate control strategies that can cope with stochastic nature of the wind [6,10].

Development of such on-line, accurate and computationally efficient coordinated control strategies for production maximisation is the aim of this paper. Particle Swarm Optimisation (PSO) is combined with a fast processing wind deficit model (TI-JM) for developing a realistic and practical on-line wind farm controller. This work is mainly based on the research carried out in [7]. This paper is structured in different sections, described as follows. A brief overview of TI-JM is given in section 2. This is followed by detailing the optimisation process in section 3 with the control problem and objective function formulation in section 3.1 and details of PSO in section 3.2. Information about the three wind farms: Brazos, SMV and Lillgrund is provided in sections 4.1, 4.2 and 4.3 respectively. The methodologies for obtaining efficiencies of the farms case studies are discussed in section 5. Results and analyses are presented in section 6. Conclusion of this work is given in section 7.

2. Turbulence Intensity based Jensen Model (TI-JM)

This section gives a brief overview of TI-JM, which is used for developing the coordinated control strategies. The detailed methodology for developing TI-JM and validation using real-time data is given in [7]. TI-JM modifies the wake decay coefficient (k) of the standard Jensen model [11,12] using wake-added turbulence intensity. Wake decay coefficient presents how quickly the wake diffuses depending upon hub height of the wake generating turbine (z) the surface roughness length (z_0) as given in equation (1) [11,12]. TI-JM has all the characteristics of the standard Jensen model [11,12] except for the constant k.

$$k = 1/[2\ln(z/z_0)] \tag{1}$$

The Jensen model has widely been used for developing farm control strategies due to its processing efficiency [2,4,7,8,13–16] and is also part of many industry standard software such as WindFarmer [7] and WindPRO [17]. Simple assumptions such as the ideal wind flow, constant k and linear wake expansion make the Jensen model computationally very efficient. However, keeping k constant means ignoring the farm-added roughness and wake-added turbulence intensity, making the model less accurate [4,18].

Wake affected turbines experience more turbulent wind as the farm acts as a roughness generator itself, because of the additional turbulence intensity [17,18]. This wake-added turbulence intensity must be considered for estimating wind speed deep inside a wind farm. TI-JM follows this principle and uses the wake added turbulence intensity along with free-stream turbulence intensity for estimating k and wind deficit inside the wind farm using equation (2). Turbulence intensity is composed of lateral,

vertical and longitudinal components. The longitudinal component (I_L) can be determined using equation (2). The wind speed deficit can now be found using equation equation (3).

$$I_L = \frac{1}{\ln(z/z_0)} = 2k \Rightarrow k = I_L/2 \tag{2}$$

$$u_x = u_0 \left[1 - \left(\frac{1-\sqrt{1-C_T}}{\left[1+\frac{k\times x}{r_0}\right]^2}\right)\right] \tag{3}$$

where u_x denotes the wind speed at distance x from the wake producing turbine, u_0 is the wind speed at the corresponding upstream turbine, r_0 is the radius of turbine swept area and C_T is the coefficient of thrust. TI-JM provides speedy and accurate results, requiring minimum parameters as inputs, which are generally easily available from SCADA data.

3. Optimisation

In order to use the controller online, an acceptable solution has to be achieved in the order of seconds so that the C_P or yaw-offset of each turbine can be calculated before the wind reaches it, as communicating these optimized values will also take some time. Coordinated control is a centralised process.

It is suggested in [3,9] that iterative algorithms can improve performance of farm controllers. Therefore, performances of different optimisation techniques (Brute Force, Genetic Algorithm, Simulated Annealing and PSO) were evaluated for wind farm coordinated control in [14], concluding that PSO can solve the coordinated control problem with high accuracy, speed and success rate as compared to other evaluated techniques.

3.1. Objective function

Net production of a wind farm is the sum of individual wind turbines' productions as given in equation (4) [2].

$$P_{Wakes} = \sum_{i=1}^{N} P_{T(i)} = \sum_{i=1}^{N} \frac{1}{2}\rho A u(i)^3 C_P(i) \cos^2\alpha_i \tag{4}$$

where (P_{Wakes}) is the total farm production, (N) shows the total number of turbines in the wind farm, $(P_{T(i)})$ is the power production of i^{th} turbine under consideration, air density is given by (ρ), turbine swept area is (A) and (α) is the yaw-offset.

Usually ρ remains constant inside the wind farm. If it is assumed that turbines in the farm have same configuration then the term $(\frac{1}{2}\rho A)$ is constant. Ignoring this constant term means that the objective function or control problem is to maximise $\sum_{i=1}^{N} u(i)^3 C_P(i) \cos^2\alpha_i$ in equation (4).

The term $(\cos^2\alpha)$ quantifies impact of yaw-offset on turbine's power production. Different exponents of $\cos\alpha$ (in equation (4)) have been used in literature [7]. The exponent of $\cos\alpha$ can fall in the range of 1 to 5 depending on the turbines and farm under consideration [7,19–23]. It is discussed in [24] that there is no physical background for the exponent of $\cos\alpha$ in equation (4) and it can be tuned for the best-fit according to the data [25]. Different exponents of $\cos\alpha$ were evaluated in [7] and it was observed that an exponent of "2" fits well with the given data, hence an exponent of "2" for $\cos\alpha$ is used in this paper.

In no-wake conditions, all the turbines experience free-steam wind speed (u_0) and there is no need to yaw i.e. $\alpha = 0°$. In this case, turbines operate with maximum C_P denoted by $(C_{P(max)})$. The aim is to get as close as possible to this maximum production in wake-affected wind conditions. In terms of a minimising objective function the aim is to minimise the difference between power production in no-wake conditions and power production in wake-affected conditions (actual production) as shown

in equation (5). As the constant ($\frac{1}{2}\rho A$) is ignored, the objective function (OF) is formulated as equation (5).

$$OF = min\left(\sum_{i=1}^{N} u_0^3 C_{P(max)} - \sum_{i=1}^{N} u(i)^3 C_P(i)\cos^2\alpha(i)\right) \quad (5)$$

The controller minimises the value in equation (5) by optimally varying C_P or α. When yaw offset is applied on an upstream turbine, the wake produced deflects away from the downstream turbine's swept area. This wake deflection is greater than the offset applied [26]. Hence wakes can be skewed away from the downstream turbine's swept area using an optimum α. Wind deficit inside the wind farm is obtained using TI-JM. The optimisation function is linked to the TI-JM using axial induction factor, which is the loss in momentum or measure of the slowing of wind speed between free stream and the rotor plane [3,27].

The relationship between α and wake skew angle (γ) given in equation (6) [26] is used in this study. This expression is developed and validated using wind tunnel experiments and real-time wind farm data [24,28,29].

$$\gamma = -1.20 \times \alpha \quad (6)$$

Equation (5) can be used for C_P and yaw based optimisation. For simplicity, C_P and yaw based optimisation will be studied independently: when optimising the C_P settings, α will be set at zero; and conversely when optimising the turbine yaw angles, C_P will be set at $C_{P(max)}$.

3.2. Particle Swarm Optimisation (PSO)

PSO consists of particles which move through the solution space in an organised way, by developing a collective intelligence for solving complex optimisation problems [30]. An individual particle represents a potential solution to the given problem. A swarm of particles represents a dimension of the objective function / control problem. Every particle's best fitness value estimated in different iterations is recorded as the local best of that specific particle. All local bests are compared with each other and the best fitness value is recorded as global best. Local and global bests along with the particles' current positions are used to estimate a velocity for finding the best possible solution [31]. This is a repetitive process which terminates when a suitable solution is acquired or number of iterations is exhausted. The number of swarms required for optimizing the objective function in equation (5) is equal to N. Power production of each turbine is a dimension of the net farm production. The value of OF in equation (5) is minimised in such a way, that each turbine's optimum C_P or α is achieved. Coordinated control process using C_P optimisation with PSO is given in Figure 1.

Preprints (www.preprints.org) | NOT PEER-REVIEWED | Posted: 8 January 2019 doi:10.20944/preprints201901.0067.v1

Peer-reviewed version available at Energies 2019, 12, 544; doi:10.3390/en12030544

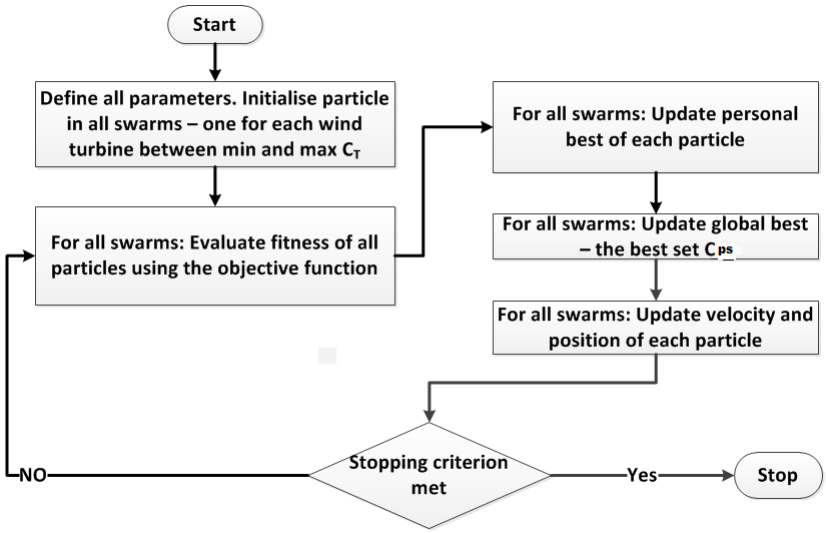

Figure 1. PSO flowchart for solving coordinated control problem

4. Wind Farms Case Studies

The Brazos, SMV and Lillgrund wind farms are used as case studies in this work. These three wind farms represent a diverse set in terms of layout, terrain and wind characteristics. A brief overview of these wind farms case studies is given as follows.

4.1. Brazos

Turbines in the Brazos wind farm are installed in a non-grid shape with downwind spacing up to 8D and crosswind spacing of as low as 2D [7]. Each row in the Brazos can be assumed as a sub-farm for faster and efficient optimisation. The encircled row in Figure 2a is used as the case study for optimisation in this work. Seven Mitsubishi MWT 1000 turbines are installed in this row with a spacing of 3D [7]. This case study is referred to Brazos-row. Brazos has flat terrain with low grass [7]. The wind-rose in Figure 2b shows the wind characteristics on site based on data from year 2004 - 2006.

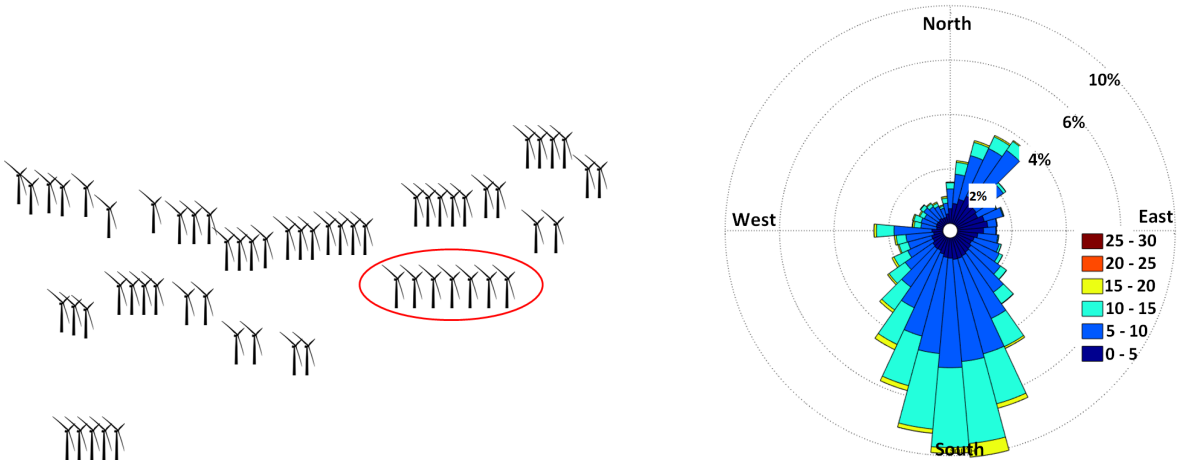

Figure 2. (**a**) Brazos layout (case study row encircled) (**b**) Wind-rose obtained with data from 2004-2006

4.2. Le Sole de Moulin Vieux (SMV)

Seven Senvion MM82 2050 kW wind turbines are installed in almost like a one-dimensional array with a spacing of 3.3D to 4.3D as depicted in Figure 3a in the SMV wind farm. SMV has a rough terrain, vegetation is present on ground. The farm has woods to the south at less than 1.5D distance. These

Preprints (www.preprints.org) | NOT PEER-REVIEWED | Posted: 8 January 2019 doi:10.20944/preprints201901.0067.v1

Peer-reviewed version available at Energies 2019, 12, 544; doi:10.3390/en12030544

woods can cause abrupt changes in wind speed and direction [8]. Figure 3b shows wind characteristics in the farm.

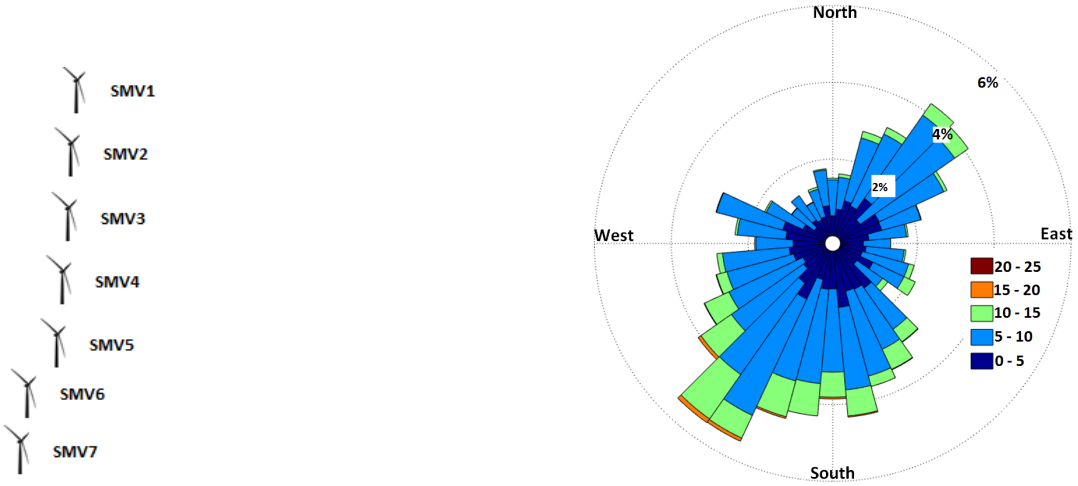

Figure 3. (a) Layout of the SMV wind farm **(b)** Wind-rose obtained with data from 2011 - 2015

4.3. Lillgrund

Lillgrund contains 48 Siemens SWT-2.3-93 turbines, installed in 8 rows as can be seen in Figure 4a. Downwind spacing is $4.5D$ while crosswind spacing is $3.5D$. Lillgrund is an offshore wind farm. The wind-rose in Figure 4b shows wind characteristics in the wind farm. Wind data of 15 years (2000-2015) was used in Figure 4b using [32] at 50m height. Performance of this wind farm is significantly affected by wakes due to the dense layout [5].

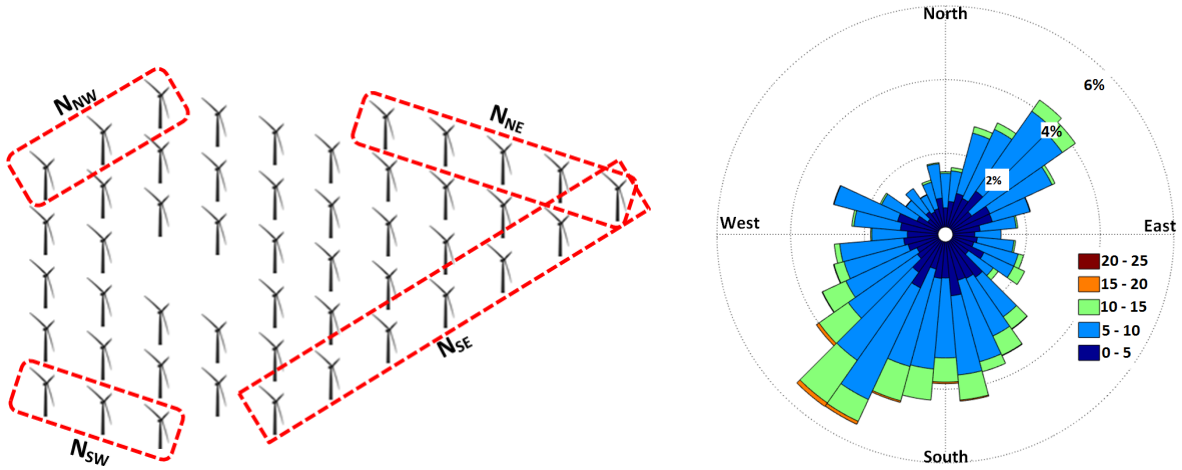

Figure 4. (a) Lillgrund layout and turbines in set j **(b)** wind-rose obtained with data from 2000-2015

5. Methodology for Calculating Efficiency

This section details the methodology for obtaining efficiencies of the three wind farms case studies. Equation (7) [2] is used for estimating efficiencies (η) of Brazos-row and SMV. The denominator (P_{max}) is simply the maximum possible farm production for a given wind speed in no-wake conditions. The numerator (P_{actual}) is the actual net production of the farm.

$$\eta = \frac{P_{actual}}{P_{max}} \tag{7}$$

Efficiency of the Lillgrund wind farm (η_{Lill}) is estimated using equation (8) [33].

Peer-reviewed version available at Energies 2019, 12, 544; doi:10.3390/en12030544

$$\eta_{Lill} = \frac{N_j}{48} \frac{\sum_{i=1}^{48} P_i}{\sum_j P_j} \tag{8}$$

where average power of the i^{th} turbine is denoted by (P_i), (j) represents a set containing a specific number of turbines (N_j) as per Table 1. The number of turbines in set j is determined using free stream wind direction. There can be four different combination in set j as it contains the turbines facing the free-stream wind, as shown in Figure 4a. Production of the j_{th} turbine in set j is given by (P_j).

Table 1. Turbines in set j

Wind Direction	Figure 4a	N_j	j
North-west	N_{NW}	3	Row-8 (3 turbines)
South-west	N_{SW}	3	Row-2 to row-4 (last turbine in each row)
North east	N_{NE}	5	Row-1 to row-5 (first turbine in each row)
South-east	N_{SE}	7	Row-1 (Seven turbines)

6. Results and Analyses

Wake effects are negligible in above-rated conditions [5], hence only below-rated conditions are assumed in the simulations in this section. Efficiencies based on WindPRO and real-time SCADA data in full or near-full wake conditions are used as benchmarks. WindPRO direction bin is kept at 10°, which is the finest possible. WindPRO uses the standard onshore and offshore values of k given in [34], for wake estimation. TI-JM uses SCADA data for Brazos-row and SMV for tuning the initial value of k according to the conditions. For TI-JM and SCADA data, the directional resolution is maintained at 1°. TI-JM is first compared with SCADA data and WindPRO using efficiencies based on greedy control. The optimal control strategies are then evaluated by comparing them with greedy control using TI-JM. Contour plots of the three wind farms case studies in full-wake conditions are used for depicting a comparison of conventional and coordinated control strategies.

Data filtering was applied to ensure that only operational turbines are analysed. It was observed that the maximum efficiency in no-wake conditions for Brazos-row and SMV wind farms was not 100%. Instead it was 82% for Brazos-row and 86% for SMV. These discrepancies may have been caused by anomalies in SCADA data or other unknown operational issues. WindPRO and TI-JM do not consider any anomalies or issues with data, taking only wake effects for wind deficit estimation. Therefore, the maximum efficiency (82% for Brazos-row and 86% for SMV) is made 100% by simply adding the difference (18% for Brazos-row, 14% for SMV) to efficiency at all points. This nullifies the impact of all other issues by taking only the impact of wake effects on farms productions. The shifted efficiency (based on SCADA data) can now be compared with efficiencies obtained with WindPRO and TI-JM.

Results and analyses for Brazos-row, SMV and Lillgrund wind farms are presented in sections 6.1, 6.2 and 6.3 respectively. These results are obtained using a basic computer (4 cores, 3.50GHz processor and 16GB RAM).

6.1. Brazos-row

Efficiency of the Brazos-row is calculated using SCADA data from 2004–2006 provided by [35]. The case study row is under wake effects in the directional sector of $90° \pm 30°$. Figure 5 depicts the average efficiency in this directional sector. The sector $90° \pm 30°$ can be further divided into bins as follows.

- Full wakes (worst case) = $90° \pm 10°$
- Partial wakes = $110° \pm 10°$ and $70° \pm 10°$

The shifted efficiency in Figure 5 shows that efficiency can drop to as low as 58% in full-wake conditions. WindPRO and TI-JM estimate that efficiency can be as low as 30% and 62% in full-wake conditions. The standard Jensen model available in WindPRO is used with a constant $k = 0.07$, for such onshore terrain. WindPRO uses the WAsP model [17] for analysing the impact of terrain on wake effects. On the other hand, TI-JM does not use any terrain model, rather it varies k according to wind conditions, instead of keeping it constant as discussed in section 2. TI-JM used k up to 0.25 for estimating wind speed deficits inside the farm. The initial value of k is the standard k for such terrains. Wind direction is derived from the data obtained from met mast.

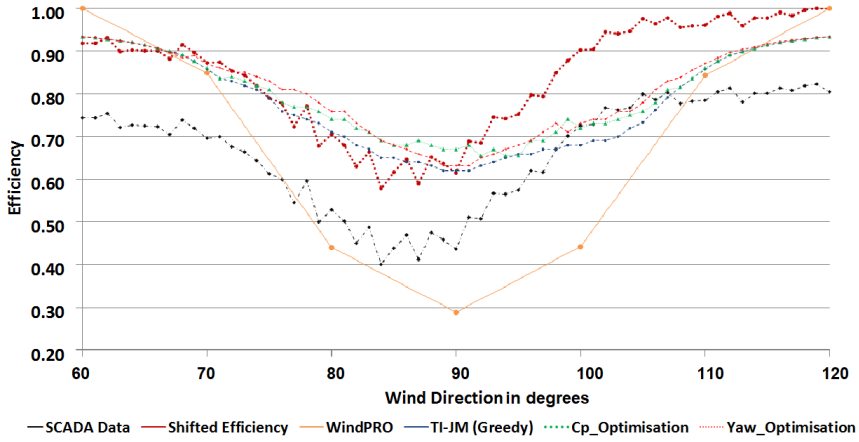

Figure 5. Brazos efficiency in $60° - 120°$ directional sector

It can be seen in Figure 5 that WindPRO and TI-JM predict almost symmetrical efficiencies around 90° as it is a straight line (row) of turbines (Figure 2a). However, the shifted efficiencies is not symmetrical on both sides of 90°. The efficiency predicted by TI-JM fits well with the shifted efficiency in the $60° - 90°$ sector. However, the efficiency is not that accurate in the $91° - 120°$ sector. Overall, TI-JM predicts better than WindPRO in most of the cases. TI-JM and WindPRO ignore wake-meandering and wind shear effects, which can result in uncertainty in models' prediction accuracy.

Both C_P and yaw-based optimised strategies can increase the average efficiency by up to 6% as compared to greedy control as can be seen in Figures 5 and 6. It was observed that coordinated control based on C_p optimisation performed better in full or near-full wake conditions. Yaw optimisation can produce better results in partial wake conditions.

The reduction in C_P of upstream turbines depends upon wind speed and direction. Optimised reduction in C_P of the upstream turbines for curtailing their power production ranges between 3% and 20%. In higher wind speeds, the C_P curtailment is minimal as wake effects are also minimal. This is true for all the three wind farms case studies. In full-wake conditions, significantly larger yaw-offset (up to $\pm 30°$) is required for deflecting the wake away from swept area of the wake affected turbines. This converts a full-wake into partial wake for the downstream turbines but at the same time significantly reduces production of the yawed turbine. A partial wake is converted into minimal or no-wake situation using a yaw-offset in a range of $\pm 15°$, producing a significant increase in wake affected turbines' productions. The impact of this yaw-offset on the yawed turbine is considerably low, hence increase in net production is observed.

Preprints (www.preprints.org) | NOT PEER-REVIEWED | Posted: 8 January 2019 doi:10.20944/preprints201901.0067.v1

Peer-reviewed version available at Energies 2019, 12, 544; doi:10.3390/en12030544

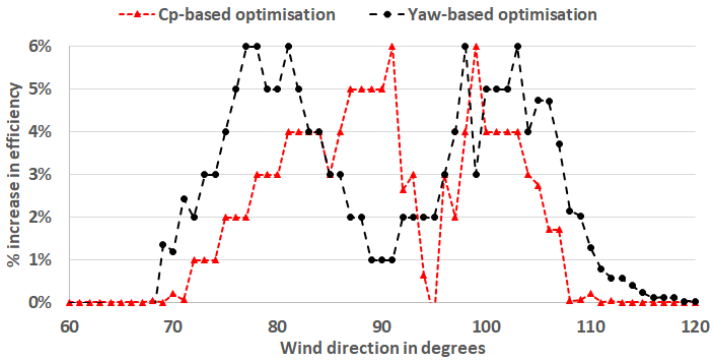

Figure 6. Impact (% increase) of optimised control strategies on Brazos-row efficiency, relative to greedy control

Wind flow with state of the art greedy control, C_P and yaw-based optimised strategies in full-wake conditions is shown in Figure 7. The lower wind speed deficit inside the wind farm with C_P optimisation, as compared to greedy control can also be seen. Figure 7c depicts the wake skewing from the downstream turbines. The wake-added turbulence intensity increases k, hence the wake spread inside the farm as shown in Figures 7. The optimisation process (in a single simulation) took less than 15 seconds for Brazos-row.

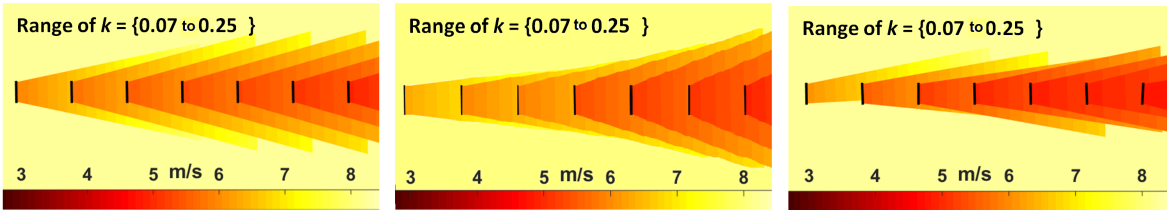

Figure 7. Comparison of control strategies for Brazos-row at 8m/s in full wakes. Range of k varies from 0.07 (free-stream) to 0.025 (deep inside the farm) **(a)** conventional greedy control **(b)** Optimised control based on C_P **(c)** Optimised control based on yaw-offset

6.2. Le Sole de Moulin Vieux (SMV)

SCADA data of the SMV wind farm from 2011–2014 is provided by Maïa Eolis (now Engie Green). Full or near-full wake conditions are assumed in the simulations. Average efficiency from the south $160^\circ - 220^\circ$ is shown in Figure 8. The sector $160^\circ - 220^\circ$ is chosen because of the prevailing wind direction and significant wake effects observed in these directions. Analyses of the SCADA data show that shifted efficiency can drop to 78% in the worst conditions. WindPRO (standard Jensen model with $k = 0.07$ and WAsP) predicted that efficiency can be as low as 70% with such layout and terrain. TI-JM estimated a minimum efficiency of 76% in the worst case. It was observed that k can increase up to 0.20 as the wind moves through the wind farm.

Preprints (www.preprints.org) | NOT PEER-REVIEWED | Posted: 8 January 2019 doi:10.20944/preprints201901.0067.v1

Peer-reviewed version available at Energies 2019, 12, 544; doi:10.3390/en12030544

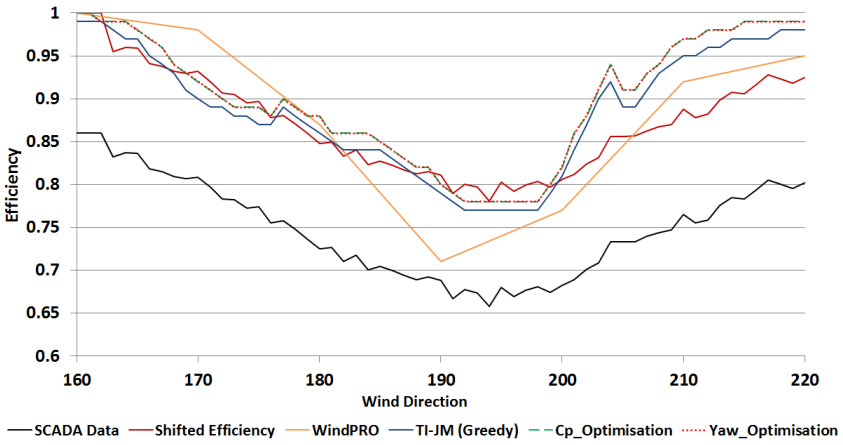

Figure 8. SMV Efficiency in $160° - 220°$ sector

It can be observed in Figure 8 that TI-JM matches the shifted efficiency better in $160° - 200°$, while WindPRO produces better results in $200° - 220°$. TI-JM under-estimates wake losses in the $200° - 220°$ sector, concluding that the k needs to be further increased in this sector for better wake estimation. Wind conditions on site due to the nearby woods (section 4.2) also adds to the complexity for wind deficit prediction.

It can be observed in Figures 8 and 9 that optimised control strategies can increase efficiency by up to 4%. The directional sector $160° - 220°$ cannot be divided into partial and full wakes for the whole wind farm in this case. Turbines in the SMV are not installed in a complete straight line (Figure 3a), hence these turbines will be under different wake conditions for a given wind direction [8]. SMV5 produces full wakes on SMV1-SMV4 in $180° \pm 10°$. For the same wind direction, SMV5 is under minimal wake effects of SMV6 and SMV6 is under negligible wake effects of SMV7. SMV6 experiences significant wake effects of SMV7 in $200° \pm 10°$ but at the same time all other turbines experiences minimal wake effects from their corresponding upstream turbines. The optimised yaw-offsets and C_P curtailment settings were the same as for Brazos-row (section 6.1).

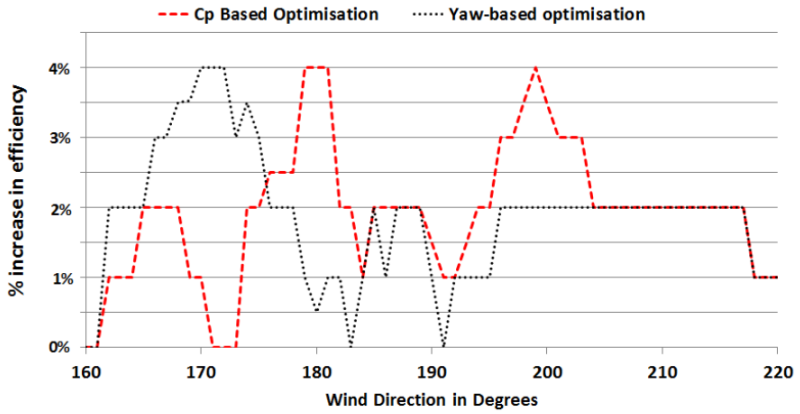

Figure 9. Impact (% increase) of optimised control strategies on SMV efficiency, relative to greedy control

A comparison of wind flow using conventional and optimised control strategies is shown in Figure 10. The optimisation process (in a single simulation) took less than 15 seconds for SMV.

Preprints (www.preprints.org) | NOT PEER-REVIEWED | Posted: 8 January 2019 doi:10.20944/preprints201901.0067.v1

Peer-reviewed version available at Energies 2019, 12, 544; doi:10.3390/en12030544

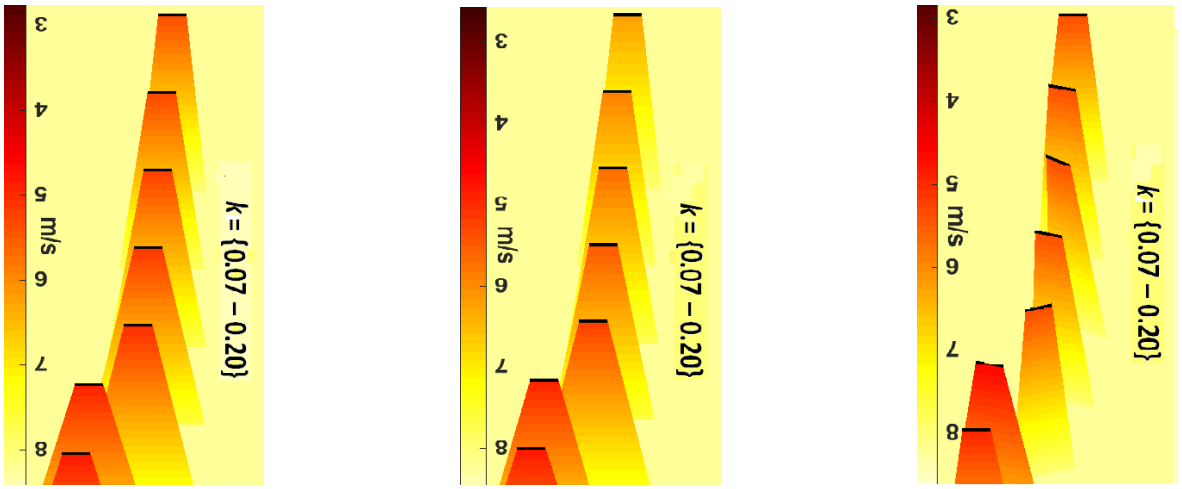

Figure 10. Comparison of control strategies for SMV at 8m/s from north. Range of k varies from 0.07 (free-stream) to 0.020 (deep inside the farm) **(a)** conventional greedy control **(b)** Optimised control based on C_P **(c)** Optimised control based on yaw-offset

6.3. Lillgrund

Lillgrund efficiency can be as low as 40% in the worst case, when turbines are under full wake effects [5]. Due to the dense layout of the farm, turbines experience wake effects in almost all wind directions. Therefore, the 360° farm efficiency curve available in [5] was digitised using [36] and reproduced in Figure 11. Other details such as farm layout, surface roughness length, turbine characteristics and turbulence intensity were provided by [33]. As per [33], the value of k shall be tuned for best fit as required by the wake model. It was noted in the simulations that values of k in equation (9) provide the best fit (for TI-JM) with actual efficiency. WindPRO used the standard $k = 0.04$ for offshore wind conditions in this case. Though WindPRO captures shape of the efficiency curve, yet in most of the cases, it underestimates wake effects. On the other hand, TI-JM predicts wake effects with almost 95% accuracy in this case.

$$\begin{aligned} k &= 0.04 \quad if \quad u_0 \leq 7.0\,m/s \\ k &= 0.08 \quad if \quad 7.0\,m/s < u_0 \leq 12.0\,m/s \\ &wind\ speeds > 12\ not\ considered\ as\ suggested\ in\ [5] \end{aligned} \tag{9}$$

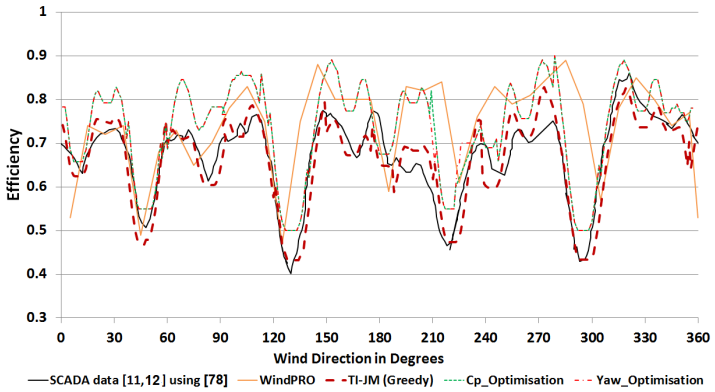

Figure 11. Average 360° efficiency of Lillgrund in below-rated conditions

Dense wind farms such as Lillgrund can significantly benefit from coordinated control. Full wake conditions are experienced when the wind flows in $45° \pm 10°, 135° \pm 10°$, $225° \pm 10°$, $315° \pm 10°$

directions. It can be seen in Figure 12 that efficiency can be improved by a maximum of 6% with optimised control strategies. It can also be observed in Figure 12 that efficiency can be increased in almost all wind directions as wake effects are always present in the farm. In partial wakes, yaw-based optimisation provides a better opportunity for efficiency improvement while C_P optimisation is more suitable in full-wake conditions. This observation is same as for Brazos-row. The ranges for C_P curtailment and yaw-offsets are same as Brazos-row and SMV.

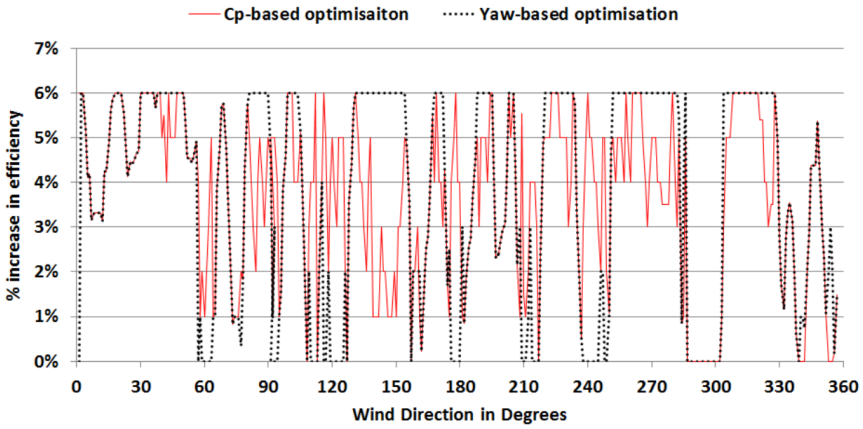

Figure 12. Impact (% increase) of optimised control strategies on Lillgrund efficiency, relative to greedy control

A comparison of wind flow using conventional and optimised control strategies is shown in Figure 13. The optimisation process (in a single simulation) took less than 50 seconds for Lillgrund.

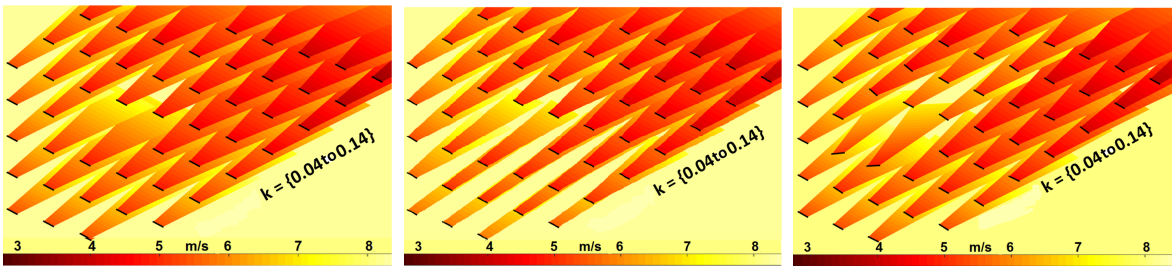

Figure 13. Comparison of control strategies for Lillgrund at 8m/s in full-wake conditions. Range of k varies from 0.04 (free-stream) to 0.14 (deep inside the farm). **(a)** conventional greedy control **(b)** Optimised control based on C_P **(c)** Optimised control based on yaw-offset

7. Conclusion

Wake-effects can have a significant impact on economic performance of wind farms by increasing production losses and fatigue loads. This work presented an intelligent and fast processing farm controller for reducing wake effects. Optimised coordinated control strategies are used for increasing farm production by optimally varying C_P or yaw-angles. The optimised control strategies uses TI-JM for estimating wind speeds inside the wind farms and PSO for optimisation. TI-JM is an improved version of the standard Jensen model. TI-JM takes deep array effect into consideration using wake added turbulence intensity for estimating k. It can accurately predict wind speed inside a wind farm in most of the cases for the wind farms case studies, hence farm production and efficiency. Both the C_P-based and yaw-based optimised strategies increased wind farm efficiency as compared to the conventional greedy control. The system has been designed for all wind conditions, however it is tested only for static wind conditions using TI-JM. Simulations confirm that average efficiency can be increased by up to 6% for Brazos-row and Lillgrund while 4% for SMV. SMV and Brazos-row were optimised in a maximum of 15 seconds while Lillgrund always took less than 50 seconds, using a basic computer. It is concluded that C_P optimisation is suitable in full-wake conditions for net production maximisation. Yaw-optimisation is beneficial for farm production maximisation in partial-wake conditions. As a future work, these results shall be validated using high fidelity wake models. It shall be noted that yaw optimisation increases fatigue loading on the yawed turbines. The aim of this paper

is only to analyse production maximisation. Fatigue load optimisation would require a multi-objective optimisation for minimising loads and maximising production of the farm, which is left for future work. Furthermore, a wind turbine has a designed service life of almost 20 to 25 years, however due to the technological advances and ever-growing size of turbines, farm operators replace these turbines much earlier than their end of life. Hence, the increase in fatigue loading for some gain in production might be economically beneficial. This can be further investigated in the future. **Author Contributions:**

This work is primarily based on the PhD research work of Tanvir Ahmad at Durham University, UK. This PhD work was supervised by Peter C. Matthews and Behzad Kazemtabrizi. Abdul Basit and Samia Akhtar provided support in the data analyses section. Juveria Anwar helped in visualization of some of the results. Olivier Coupiac provided assistance in using WindPRO and obtaining data for the Lillgrund wind farm.

Funding: The PhD research was funded by the Commonwealth Scholarship Commission (CSC), UK (reference: PKCS-2013-384). Pakistan Council of Renewable Energy Technologies (PCRET) funded this publication jointly with the US Pakistan Center for Advanced Studies in Energy, University of Engineering & Technology Peshawar, Pakistan.

Conflicts of Interest: "The authors declare no conflict of interest."

Abbreviations

The following abbreviations are used in this manuscript:

PSO	Particle Swarm Optimisation
TI-JM	Turbulence Intensity based Jensen Model
SMV	Le Sole de Moulin Vieux

1. Bitar, E.; Seiler, P. Coordinated control of a wind turbine array for power maximization. American Control Conference (ACC). IEEE, 2013, pp. 2898–2904.
2. Pao, L.Y.; Johnson, K.E. A tutorial on the dynamics and control of wind turbines and wind farms. American Control Conference, ACC'09; IEEE: 172, 2009; pp. 2076–2089.
3. Johnson, K.E.; Thomas, N. Wind farm control: addressing the aerodynamic interaction among wind turbines. American Control Conference, ACC'09; IEEE: 155, 2009; pp. 2104–2109.
4. Ahmad, T.; Girard, N.; Kazemtabrizi, B.; Matthews, P. Analysis of two onshore wind farms with a dynamic farm controller. EWEA, Paris France, 2015.
5. Dahlberg, J.A. Assessment of the Lillgrund windfarm: Power performance. Technical Report 21858-1, Vatenfall, Vindkraft AB, 2009.
6. Aranda, F.A. Wind Farm Control Methods, IEA R&D Wind Task 11 - Topical Expert Meeting. Technical report, International Energy Agency, 2012.
7. Ahmad, T. Wind Farm Coordinated Control and Optimisation. PhD thesis, School of Engineering & Computing Sciences, Durham University UK, 2017. Availalble online at [http://etheses.dur.ac.uk/12323/1/Tanvir_Thesis_Final_Submission.pdf].
8. Ahmad, T.; Coupiac, O.; Pettit, A.; Guignard, S.; Girard, N.; Kazemtabrizi, B.; Matthews, P. Field Implementation and Trial of Coordinated Control of Wind Farms. *IEEE Transactions on Sustainable Energy* **2017**.
9. Ambekar, A.; Ryali, V.; Tiwari, A.K. Methods and systems for optimizing farm-level metrics in a wind farm, 2015. US Patent 9,201,410.
10. Soleimanzadeh, M.; Wisniewski, R.; Kanev, S. An optimization framework for load and power distribution in wind farms. *Journal of Wind Engineering and Industrial Aerodynamics* **2012**, *107*, 256–262.
11. Jensen, N.O. A note on wind generator interaction. Technical Report Risø -M-2411, Risø National Laboratory, Roskilde, Denmark, 1983.
12. Katic, I.; Højstrup, J.; Jensen, N.O. A simple model for cluster efficiency. European Wind Energy Association Conference and Exhibition, 1986, pp. 407–410.
13. Park, J.; Kwon, S.; Law, K.H. Wind farm power maximization based on a cooperative static game approach. SPIE Smart Structures and Materials+ Nondestructive Evaluation and Health Monitoring. International Society for Optics and Photonics, 2013, pp. 86880R–86880R.

14. Ahmad, T.; Matthews, P.; Kazemtabrizi, B. PSO Based Wind Farm Controller. The 11th edition of the International Conference on Evolutionary and Deterministic Methods for Design, Optimization and Control with Applications to Industrial and Societal Problems, EUROGEN-2015 Glasgow, UK, 2015, pp. 277–283.
15. González, J.S.; Payán, M.B.; Santos, J.R.; Rodríguez, Á.G.G. Maximizing the overall production of wind farms by setting the individual operating point of wind turbines. *Renewable Energy* **2015**, *80*, 219–229.
16. Marden, J.R.; Ruben, S.D.; Pao, L.Y. Surveying game theoretic approaches for wind farm optimization. Proceedings of the AIAA aerospace sciences meeting, 2012, pp. 1–10.
17. Nielsen, P.; Villadsen, J.; Kobberup, J.; Madsen, P.; Jacobsen, T.; Thøgersen, M.L.; Sørensen, M.V.; Sørensen, T.; Svenningsen, L.; Motta, M.; Bredelle, K.; Funk, R.; Chun, S.; Ritter, P. *WindPRO 2.7 User Guide*. EMD International A/S, Aalborg, Denmark, 3rd ed., 2010.
18. Annoni, J.; Gebraad, P.M.; Scholbrock, A.K.; Fleming, P.A.; van Wingerden, J.W. Analysis of axial-induction-based wind plant control using an engineering and a high-order wind plant model. *Wind Energy* **2015**, *19*, 1135–1150.
19. Knudsen, T.; Bak, T.; Svenstrup, M. Survey of wind farm control power and fatigue optimization. *Wind Energy* **2014**.
20. Qian, G.W.; Ishihara, T. A New Analytical Wake Model for Yawed Wind Turbines. *Energies* **2018**, *11*, 665.
21. Marathe, N.; Swift, A.; Hirth, B.; Walker, R.; Schroeder, J. Characterizing power performance and wake of a wind turbine under yaw and blade pitch. *Wind Energy* **2016**, *19*, 963–978.
22. Wan, S.; Cheng, L.; Sheng, X. Effects of yaw error on wind turbine running characteristics based on the equivalent wind speed model. *Energies* **2015**, *8*, 6286–6301.
23. Park, J.; Law, K.H. A data-driven, cooperative wind farm control to maximize the total power production. *Applied Energy* **2016**, *165*, 151–165.
24. Boorsma, K. Power and loads for wind turbines in yawed conditions. Technical report, ECN-E-12-047, ECN, Petten, The Netherlands, 2012.
25. Annoni, J.; Fleming, P.; Scholbrock, A.; Roadman, J.; Dana, S.; Adcock, C.; Porte-Agel, F.; Raach, S.; Haizmann, F.; Schlipf, D. Analysis of Control-Oriented Wake Modeling Tools Using Lidar Field Results.
26. Wagenaar, J.; Machielse, L.; Schepers, J. Controlling wind in ECN scaled wind farm. *Proc. Europe Premier Wind Energy Event* **2012**, pp. 685–694.
27. Corten, G.; Schaak, P.; Bot, E. More power and less loads in wind farms: Heat and Flux. European Wind Energy Conference & Exhibition, London, UK, 2004.
28. Schram, C.; Vyas, P. Windpark turbine control system and method for wind condition estimation and performance optimization, 2005. US Patent App. 11/288,081.
29. Kanev, S.; Savenije, F. Active Wake Control: loads trends. Technical Report ECN-E–15-004, ECN, Petten, The Netherlands, 2015.
30. Kennedy, J.; Spears, W.M. Matching algorithms to problems: an experimental test of the particle swarm and some genetic algorithms on the multimodal problem generator. Proceedings of the IEEE international conference on evolutionary computation. Citeseer, 1998, pp. 78–83.
31. Kennedy, J.; Eberhart, R. Particle swarm optimization. Proceedings of IEEE international conference on neural networks; Perth, Australia: 162, 1995; Vol. 4, pp. 1942–1948.
32. Rienecker, M.M.; Suarez, M.J.; Gelaro, R.; Todling, R.; Bacmeister, J.; Liu, E.; Bosilovich, M.G.; Schubert, S.D.; Takacs, L.; Kim, G.K.; others. MERRA: NASA's modern-era retrospective analysis for research and applications. *Journal of Climate* **2011**, *24*, 3624–3648.
33. Moriarty, P.; Rodrigo, J.S.; Gancarski, P.; Chuchfield, M.; Naughton, J.W.; Hansen, K.S.; Machefaux, E.; Maguire, E.; Castellani, F.; Terzi, L.; others. IEA-Task 31 WAKEBENCH: Towards a protocol for wind farm flow model evaluation. Part 2: Wind farm wake models. Journal of Physics: Conference Series. IOP Publishing, 2014, Vol. 524, p. 012185.
34. Thørgersen, M.; Sørensen, T.; Nielsen, P.; Grötzner, A.; Chun, S. *WindPRO/PARK: Introduction to wind turbine wake modelling and wake generated turbulence*. EMD International A/S, Niels Jernesvej 10, 9220 Aalborg, 2005. Available at: http://www.emd.dk/files/windpro/manuals/for_print/Appendices-all_UK.pdf.
35. Bueno Gayo, J. ReliaWind Project Final Report. Technical Report Project Nr 212966, Gamesa Innovation and Technology, 2011.
36. Rohatgi, A. WebPlotDigitizer. online. http://arohatgi.info/WebPlotDigitizer/ Accessed January 8, 2019.